

## Oligomeric $\beta\beta\alpha$ Miniprotein Motifs: Pivotal Role of Single Hinge Residue in Determining the Oligomeric State

Kevin A. McDonnell and Barbara Imperiali\*

Contribution from the Department of Chemistry, Massachusetts Institute of Technology, Cambridge, Massachusetts 02139

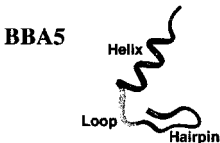
Received September 1, 2001

**Abstract:** The role of a single glycine hinge residue in the structure of **BBAT1**, a  $\beta\beta\alpha$  peptide that forms a discrete homotrimeric structure in solution, was evaluated with 11 new peptide sequences which differ only in the identity of the residue at the hinge position. The integrity of the structure and oligomeric state of the peptides was evaluated by using a combination of analytical ultracentrifugation and circular dichroism spectroscopy. Initially, it was discovered that the glycine hinge adopts backbone dihedral angles favored in D-amino acids and that incorporation of D-alanine at the hinge position stabilizes the trimer species. Subsequently, the effect of the side chains of different D-amino acids at the hinge position was evaluated. While incorporation of polar amino acids led to a destabilization of the oligomeric form of the peptide, only peptides including D-Ser or D-Asp at the hinge position were able to achieve a discrete trimer species. Incorporation of hydrophobic amino acids D-Leu and D-Phe led to oligomerization beyond a trimer to a tetrameric form. The dramatic differences among the thermodynamic stabilities and oligomeric states of these peptides illustrates the pivotal role of the hinge residue in the oligomerization of the  $\beta\beta\alpha$  peptides.

### Introduction

In developing peptide scaffolds for the incorporation of novel catalytic function, we have observed that many of the small constructs that are accessible by de novo design methods are too small (20–40 amino acids) to properly accommodate the components necessary to achieve enhanced catalytic function.<sup>1–3</sup> The generation of slightly larger “miniproteins” would require either the chemical synthesis of longer peptides, which can be inefficient, or the expression of the longer sequences, which would limit the use of nonencoded synthetic amino acids. Native chemical ligation can also be used in conjunction with both chemical synthesis and expression systems to achieve medium and larger sized protein scaffolds.<sup>4,5</sup> An alternative strategy to access miniprotein structures that incorporate nonnatural amino acids is to design short synthetic peptide sequences which are capable of forming stable oligomeric structures. Such a strategy would allow access to a range of miniprotein structures of different sizes that might be used as scaffolds for the construction of functional motifs. Currently, there has been a great deal of success in designing oligomeric peptide structures from  $\alpha$ -helical peptides,<sup>6–9</sup> however, the development of discrete  $\beta$

Table 1. Sequences of **BBA5** and **BBAT1**



Peptide	Hairpin	Loop/ Hinge	Helix
<b>BBA5</b>	Ac-YRVpSYDF	SRS	DELAKLLRQHAG-NH <sub>2</sub>
<b>BBAT1</b>	Ac-YRIpSYDF	G	DELAKLLRQADapBzG-NH <sub>2</sub>

Lower case indicates D-amino acid

or mixed  $\alpha\beta$  oligomeric peptide structures has been more challenging.<sup>10–12</sup> Access to these alternate oligomeric structures would greatly expand the repertoire of synthetic peptide scaffolds for the generation of functional peptides and would provide insight into the forces that mediate protein–protein interactions.

Recently, we reported the discovery and characterization of a peptide, **BBAT1**, that forms a discrete homotrimeric structure in aqueous solution.<sup>13,14</sup> The sequence of **BBAT1** was based on **BBA5**, a monomeric  $\beta\beta\alpha$  peptide<sup>15–17</sup> previously designed in this group. **BBA5** consists of three elements of secondary structure: an  $\alpha$ -helix, a  $\beta$ -hairpin, and a loop that connects the helix and hairpin. **BBAT1** differs from **BBA5** in only three elements of primary sequence (see Table 1), the major change

(1) Shogren-Knaak, M. A.; Imperiali, B. *Bioorg. Med. Chem. Lett.* **1999**, *7*, 11993–2002.  
 (2) McDonnell, K. A. *Towards Incorporation of Catalytic Function into Small Folded Peptide Scaffolds*; MIT: Cambridge, 2001.  
 (3) Corey, M. J.; Corey, E. *Proc. Natl. Acad. Sci. U.S.A.* **1996**, *93*, 11428–11434.  
 (4) Dawson, P. E.; Muir, T. W.; Clarkelewis, I.; Kent, S. B. H. *Science* **1994**, *266*, 776–779.  
 (5) Dawson, P. E.; Kent, S. B. H. *Annu. Rev. Biochem.* **2000**, *69*, 923–960.  
 (6) DeGrado, W. F.; Summa, C. M.; Pavone, V.; Nastri, F.; Lombardi, A. *Annu. Rev. Biochem.* **1999**, *68*, 779–819.  
 (7) Micklatlcher, C.; Chmielewski, J. *Curr. Opin. Chem. Biol.* **1999**, *3*, 724–729.

(8) Skalicky, J. J.; Gibney, B. R.; Rabanal, F.; Urbauer, R. J. B.; Dutton, P. L.; Wand, A. J. *J. Am. Chem. Soc.* **1999**, *121*, 4941–4951.  
 (9) Hill, R. B.; DeGrado, W. F. *J. Am. Chem. Soc.* **1998**, *120*, 1138–1145.  
 (10) Mayo, K. H.; Ilyina, E. *Protein Sci.* **1998**, *7*, 358–368.  
 (11) Ilyina, E.; Roongta, V.; Mayo, K. H. *Biochemistry* **1997**, *36*, 5245–5250.

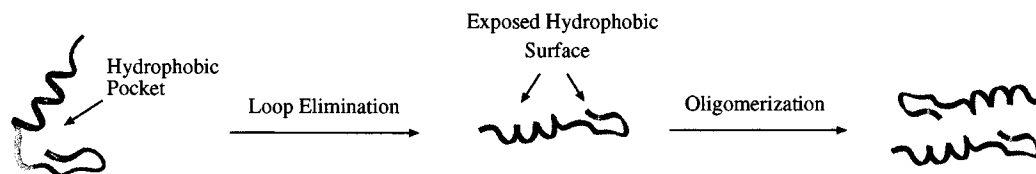


**Figure 1.** Strategy for inducing oligomerization of  $\beta\beta\alpha$  motif peptides.

being a truncation of the three-membered loop to a single amino acid hinge. The tripeptide loop, Ser-Arg-Ser, allows the helix and hairpin of **BBA5** to interact with each other via discrete hydrophobic contacts.<sup>15,16</sup> The shorter, single glycine hinge of **BBAT1** appears to prevent the intramolecular interaction between the hairpin and the helix thereby favoring oligomerization of the peptide to bury the exposed hydrophobic surfaces, as illustrated schematically in Figure 1. The other sequence changes include replacement of Val with Ile in position 3 in the  $\beta$ -hairpin, and substitution of the His-Ala dipeptide at the N-terminus of the helix with Ala-DapBz, where DapBz is an unnatural amino acid consisting of  $\alpha,\beta$ -diaminopropionic acid derivatized with a benzoyl functionality on the side chain nitrogen. This unusual amino acid is a remnant of the fluorescent screening process utilized to identify the **BBAT1** sequence.<sup>13</sup>

After evaluating substitutions at various positions in the sequence of **BBAT1**, it was determined that the hinge position was the most interesting and had the greatest influence on the oligomeric state.<sup>2,13</sup> In preliminary experiments, the hinge length and precise identity appeared to be major determinants in the formation of discrete oligomeric assemblies.<sup>13</sup> To better understand the role of the hinge residue in controlling the oligomeric state of **BBAT1**, we have synthesized eleven peptides with different residues at the hinge position and explored their structures by analytical ultracentrifugation (AUC) and circular dichroism (CD). These new peptide sequences incorporate amino acids with different conformational preferences and side chains of different functionalities (polar, nonpolar, charged, neutral). Biophysical studies reveal that the hinge residue plays a key role in determining the oligomeric state of the peptides.

## Experimental Procedures

**Peptide Synthesis.** Fmoc-protected amino acids for solid-phase peptide synthesis were obtained from PE Biosystems, Novabiochem or Bachem. Peptides were synthesized on an Advanced Chemtech 396 $\Omega$  automated synthesizer at a 0.04 mmol scale. Fmoc-PAL-PEG-PS (PE Biosystems) resin (0.18 mmol/g) was used to afford carboxyl-terminal primary amides. Couplings were performed at a concentration of 0.15 M acylating reagent ( $\sim$ 6-fold excess) with in situ *O*-benzotriazolyl-*N,N,N',N'*-tetramethyluronium hexafluoro-phosphate (HBTU)/hydroxybenzotriazole (HOBt)/diisopropylethylamine (DIPEA) activation. Each residue was coupled twice for 45 min followed by a 10 min reaction with acetic anhydride and HOBt in DMF/DCM to cap any unreacted amines. Fmoc deprotection was performed with piperidine (20% in DMF). After addition of the final residue, the amino terminus was acetyl-capped and the resin was rinsed with DCM then dried.

$\alpha,\beta$ -Diaminopropionic acid (Dap) amino acid was incorporated as Fmoc-L-Dap(alloc)-OH (Bachem). The allyloxycarbonyl side chain protecting group (alloc) can be selectively removed prior to deprotection of the peptide and cleavage from the resin. The removal of this group is described below. The free  $\beta$ -amine was coupled to benzoic acid by using in situ HBTU/HOBt/DIPEA activation to generate the DapBz residue.

The removal of the alloc group was achieved following reported conditions.<sup>18</sup> A typical procedure is as follows: Following peptide synthesis, the dry resin was placed in a stoppered vial under a blanket of nitrogen. The resin was swollen in 3 mL of dry, distilled DCM for 5 min, then 25 equiv of phenylsilane was added. After 3 min, 0.2 equiv of tetrakis(triphenylphosphine)palladium was dissolved in 2 mL of dry distilled DCM and added to the resin under nitrogen. The vial was capped, shielded from light, and agitated on a wrist-action shaker at low speed for 2 h. The resin was then filtered and rinsed with DCM (5  $\times$  10 mL), DMF (5  $\times$  10 mL), and then a palladium chelating cocktail (DMF/diethyldithiocarbamic acid $\cdot$ 3H<sub>2</sub>O/triethylamine, 25 mL:225 mg:250  $\mu$ L). Traces of this solution were removed with a basic wash (0.5% v/v triethylamine in DMF), DMF (5  $\times$  10 mL), and a final wash with methanol. The resin was then dried under reduced pressure.

The final peptide deprotection and cleavage from the resin was achieved with 5 mL of 95:2.5:2.5 TFA:H<sub>2</sub>O:triisopropylsilane for 2 h. The resin was filtered and the filtrate concentrated to ca. 1 mL volume after which the crude peptides were precipitated and triturated with cold 1:1 ether:hexanes. The supernatant was decanted and crude peptides were dissolved in water with a minimal amount of acetonitrile then frozen and lyophilized to dryness. The lyophilized crude peptides were dissolved in water and purified by preparative reverse phase HPLC (RP-HPLC) (YMC Prep Column/Waters HPLC/linear gradient 20–50% acetonitrile (0.1% TFA)/H<sub>2</sub>O (0.1% TFA) over 25 min). Peptide identities were confirmed by electrospray ionization mass spectroscopy on a PE-Biosystems Mariner TOF instrument: **1** (C<sub>127</sub>H<sub>194</sub>N<sub>36</sub>O<sub>37</sub>) calcd 2815.4, obsd 2816.2; **2** (C<sub>118</sub>H<sub>177</sub>N<sub>31</sub>O<sub>33</sub>) calcd 2556.3, obsd 2557.0; **3** (C<sub>118</sub>H<sub>177</sub>N<sub>31</sub>O<sub>33</sub>) calcd 2556.3 obsd 2556.7; **4** (C<sub>118</sub>H<sub>177</sub>N<sub>31</sub>O<sub>33</sub>) calcd 2556.3 obsd 2556.7; **5** (C<sub>119</sub>H<sub>178</sub>N<sub>32</sub>O<sub>34</sub>) calcd 2599.3, obsd 2600.1; **6** (C<sub>118</sub>H<sub>177</sub>N<sub>31</sub>O<sub>34</sub>) calcd 2572.3, obsd 2573.0; **7** (C<sub>119</sub>H<sub>177</sub>N<sub>31</sub>O<sub>35</sub>) calcd 2600.3 obsd 2601.1; **8** (C<sub>121</sub>H<sub>184</sub>N<sub>34</sub>O<sub>33</sub>) calcd 2641.4, obsd 2642.1; **9** (C<sub>118</sub>H<sub>178</sub>N<sub>32</sub>O<sub>33</sub>) calcd 2571.3, obsd 2572.1; **10** (C<sub>121</sub>H<sub>183</sub>N<sub>31</sub>O<sub>33</sub>) calcd 2598.4, obsd 2599.1; **11** (C<sub>124</sub>H<sub>181</sub>N<sub>31</sub>O<sub>33</sub>) calcd 2632.3, obsd 2632.9.

Peptide stock solutions were prepared with use of MilliQ H<sub>2</sub>O. The concentrations of the stock solutions were determined in 6 M guanidine $\cdot$ HCl (Gdn $\cdot$ HCl) by UV-vis spectroscopy. The absorbance at 280 nm of a 1:100 dilution of stock solution in the Gdn $\cdot$ HCl was measured and the concentration calculated by using reported extinction coefficients for tyrosine (1285 M<sup>-1</sup> cm<sup>-1</sup> @ 280 nm) and tryptophan (5685 M<sup>-1</sup> cm<sup>-1</sup> @ 280 nm)<sup>19</sup> and an extinction coefficient for DapBz experimentally determined (435 M<sup>-1</sup> cm<sup>-1</sup> @280 nm).

**Analytical Ultracentrifugation.** Equilibrium sedimentation experiments were performed on a Beckman XL-I analytical ultracentrifuge equipped with an AN60TI rotor and a 6-sector Epon centerpiece with quartz windows. Aqueous peptide stocks were diluted into phosphate buffer (50 mM, pH 7.0) to the desired concentrations. These samples

(12) Quinn, T. P.; Tweedy, N. B.; Williams, R. W.; Richardson, J. S.; Richardson, D. C. *Proc. Natl. Acad. Sci. U.S.A.* **1994**, *91*, 8747–8751.  
 (13) Mezo, A. R.; Cheng, R. P.; Imperiali, B. *J. Am. Chem. Soc.* **2001**, *123*, 3885–3891.  
 (14) Mezo, A. R.; Ottesen, J. J.; Imperiali, B. *J. Am. Chem. Soc.* **2001**, *123*, 1002–1003.  
 (15) Struthers, M. D.; Cheng, R. P.; Imperiali, B. *Science* **1996**, *271*, 342–345.  
 (16) Struthers, M. D.; Cheng, R. P.; Imperiali, B. *J. Am. Chem. Soc.* **1996**, *118*, 3073–3081.  
 (17) Struthers, M.; Ottesen, J. J.; Imperiali, B. *Fold. Des.* **1998**, *3*, 95–103.

(18) Peluso, S.; Dumy, P.; Nkubana, C.; Yokokawa, Y.; Mutter, M. *J. Org. Chem.* **1999**, *64*, 7114–7120.  
 (19) Pace, C. N.; Vajdos, F.; Fee, L.; Grimsley, G.; Gray, T. *Protein Sci.* **1995**, *4*, 2411–2423.

**Table 2.** Sequences of **BBAT1** and Hinge Mutants<sup>a</sup>

Peptide	Sequence
<b>BBAT1</b>	Ac-YRIpSYDF <b>G</b> DELAKLLRQADapBzG-NH <sub>2</sub>
<b>1</b>	Ac-YRIpSYDF <b>SRS</b> DELAKLLRQADapBzG-NH <sub>2</sub>
<b>2</b>	Ac-YRIpSYDF <b>β</b> DELAKLLRQADapBzG-NH <sub>2</sub>
<b>3</b>	Ac-YRIpSYDF <b>A</b> DELAKLLRQADapBzG-NH <sub>2</sub>
<b>4</b>	Ac-YRIpSYDF <b>a</b> DELAKLLRQADapBzG-NH <sub>2</sub>
<b>5</b>	Ac-YRIpSYDF <b>n</b> DELAKLLRQADapBzG-NH <sub>2</sub>
<b>6</b>	Ac-YRIpSYDF <b>s</b> DELAKLLRQADapBzG-NH <sub>2</sub>
<b>7</b>	Ac-YRIpSYDF <b>d</b> DELAKLLRQADapBzG-NH <sub>2</sub>
<b>8</b>	Ac-YRIpSYDF <b>r</b> DELAKLLRQADapBzG-NH <sub>2</sub>
<b>9</b>	Ac-YRIpSYDF <b>dap</b> DELAKLLRQADapBzG-NH <sub>2</sub>
<b>10</b>	Ac-YRIpSYDF <b>l</b> DELAKLLRQADapBzG-NH <sub>2</sub>
<b>11</b>	Ac-YRIpSYDF <b>f</b> DELAKLLRQADapBzG-NH <sub>2</sub>

<sup>a</sup> Lower case indicates D-amino acid. Position 9 noted in bold.  $\beta$  =  $\beta$ -aminopropionic acid, **Dap** =  $\alpha,\beta$ -diaminopropionic acid.

were then loaded into the centerpiece. For each sample, a blank cell was loaded with a matching sample of phosphate buffer, with distilled water replacing the volume of peptide stock added. Acquisition of the absorption scans was performed in triplicate at 5 °C at wavelengths from 220 to 315 nm. For the purposes of comparison, the experimental parameters used to examine the peptides were consistent with those used to examine the first generation of oligomeric peptides.<sup>14</sup> Samples were equilibrated at 45 000 rpm for 18 h. Data collected at 15 and 18 h indicated that samples had reached equilibrium. Absorption distributions were analyzed in KaleidaGraph software, version 3.0.5 and NONLIN, Mac Version (beta).<sup>20–22</sup> Data were fitted to a single ideal species model where the partial specific volume was calculated and the solution density was based on the buffer concentration. The plot of radius<sup>2</sup> versus the natural log of absorption was fit to a linear curve to determine the reduced molecular weight ( $\sigma$ ).<sup>23</sup> In NONLIN, the raw absorption data were fit by using a nonlinear least-squares analysis to determine  $\sigma$ . The aggregate molecular weight ( $M$ ) of the peptide species in solution was determined by using calculated partial specific volumes ( $\bar{v}$ ) and buffer densities ( $\rho$ ) in eq 1. In cases where the fit to the linear

$$M = \frac{\sigma^* RT}{(1 - \bar{v}^* \rho) \omega^2} \quad (1)$$

curve was good ( $R \geq 0.999$ ) and the values of  $\sigma$  determined by both the linear fit and the NONLIN fit were in good agreement, the peptide species is designated as a single species in Table 3.

**Circular Dichroism Spectroscopy.** Circular dichroism experiments were performed on an Aviv Model 202 CD spectrometer. Samples were prepared by dilution of peptide stocks to concentrations between 1 and 500  $\mu$ M in phosphate buffer (50 mM, pH 7.0). Concentration-dependent measurements were performed at 5 °C in a 0.1 or 1.0 cm path length quartz cell. Temperature-dependent measurements were performed in a 0.1 cm path length quartz cell between 5 and 80 °C. In all experiments the optical chamber was continually flushed with dry N<sub>2</sub> gas. Scans were collected in the range from 195 to 300 nm, with a bandwidth of 1.0 nm, a scan speed of 50 nm/min, a time constant of 0.5 s, and a

**Table 3.** AUC Data for **BBAT1** and Peptides **1–11**<sup>a</sup>

peptide	hinge sequence	concn. ( $\mu$ M)	oligomeric state	single species
<b>BBAT1</b>	Gly	500	3.19	Y
		1000	3.12	Y
<b>1</b>	Ser-Arg-Ser	50	1.10	Y
		500	1.70	N
<b>2</b>	$\beta$ -Ala	250	2.00	N
<b>3</b>	Ala	100	2.30	N
<b>4</b>	D-Ala	20	2.98	Y
		200	3.29	Y
		1000	3.12	Y
<b>5</b>	D-Asn	100	1.3	N
<b>6</b>	D-Ser	100	2.93	N
		500	3.01	Y
<b>7</b>	D-Asp	20	1.05	Y
		100	2.10	N
		500	3.16	Y
<b>8</b>	D-Arg	100	1.36	N
		500	1.59	N
<b>9</b>	D-Dap	100	1.14	N
		500	1.80	N
<b>10</b>	D-Leu	20	4.13	N
		100	4.45	N
		500	4.67	N
<b>11</b>	D-Phe	20	3.90	Y
		100	3.72	Y
		500	4.02	Y

<sup>a</sup>  $\beta$ -Ala =  $\beta$ -aminopropionic acid, **Dap** =  $\alpha,\beta$ -diaminopropionic acid.

scan resolution of 0.25 nm. Three accumulations per sample were performed for concentration-dependent measurements and one accumulation every 5 °C for temperature-dependent experiments. CD spectra were analyzed in KaleidaGraph software, version 3.0.5, and are reported in (deg  $\times$  cm<sup>2</sup>)/(dmol  $\times$  amide bonds).

## Results

Eleven new peptides were synthesized which differed from **BBAT1** only at the hinge position (Table 2) that connects the  $\alpha$  and  $\beta$  elements of secondary structure. Analytical ultracentrifugation was used as the primary screening tool to determine the effect these sequence changes had on the oligomeric state of the peptide. The AUC data for peptides **1–11** are listed in Table 3. The oligomeric state for each peptide was determined by dividing the aggregate weight average molecular weight, determined by AUC, by the actual molecular weight of the monomeric peptide.

**Role of Loop Length and Hinge Conformation.** Peptides **1–4** were designed to evaluate the role of the loop length and hinge conformation. Peptide **1** included the original **BBA5** loop sequence, Ser-Arg-Ser, in place of the single amino acid glycine of **BBAT1**. Interestingly, although this peptide exhibits a moderate amount of aggregation at 500  $\mu$ M, it behaves as a single, monomeric species at 50  $\mu$ M. This result indicates that while the loop truncation was the most significant factor in promoting oligomerization, the other two modifications to the **BBA5** sequence also contribute to the formation of the resulting stable trimeric form of **BBAT1**. The specific roles of these two sequence alterations in the oligomeric structure are also currently under investigation. Peptides **2**, **3**, and **4** included three amino acids at position 9 that differ from glycine by only a single methylene (Figure 2). Peptide **2** incorporates a  $\beta$ -aminopropionic acid ( $\beta$ -alanine) residue, while peptides **3** and **4** incorporate L- or D-alanine, respectively. The AUC data from these peptides reveal that even such a minor alteration in the chemical

(20) Yphantis, D. A. *Biochemistry* **1964**, *3*, 297–317.

(21) Johnson, M. L.; Correia, J. J.; Yphantis, D. A.; Halvorson, H. R. *Biophys. J.* **1981**, *36*, 575–588.

(22) NONLIN; Available via anonymous FTP transfer from the RASMB network; ftp://rasmb.bbri.org/rasmb/rasmb\_homepage.html.

(23) Harding, S. E.; Rowe, A. J.; Horton, J. C. *Analytical Ultracentrifugation in Biochemistry and Polymer Science*; Royal Society of Chemistry: Oxford, 1992.

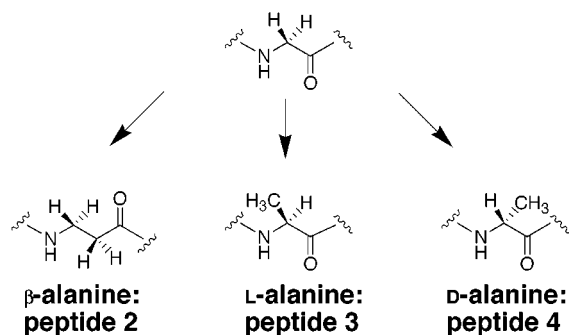


**Figure 2.** Structures of loop residues of **BBAT1** and peptides 2–4.

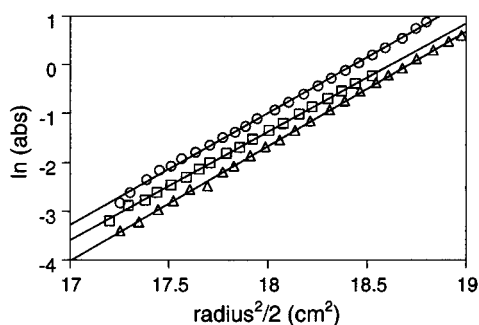


**Figure 3.** AUC data for peptide **4** (D-Ala) at 20  $\mu\text{M}$  (○), 200  $\mu\text{M}$  (□), and 1000  $\mu\text{M}$  (Δ). The data are shown fit to a single ideal species model where  $\ln(\text{abs})$  vs  $r^2/2$  yields a straight line. Absorbance was monitored at 234 (20  $\mu\text{M}$ ), 282 (200  $\mu\text{M}$ ), and 293 nm (1000  $\mu\text{M}$ ).

composition of the hinge region of the **BBAT1** peptide has dramatic effects on the integrity of the quaternary structure.

Peptide **2**, which incorporates  $\beta$ -Ala, was insoluble beyond 250  $\mu\text{M}$ . At that concentration, the peptide exists as a mixture of species of average MW 5152.30 ( $2.0 \times$  monomer). It appears that even such a small increase in the length of the loop has a detrimental effect on the ability of the peptide to form stable oligomers. Most likely, the  $\beta$ -Ala does not stabilize a conformation that enables the adequate burial of the hydrophobic groups on the peptide in the oligomeric state, resulting in uncontrolled aggregation and precipitation. A similar result was observed with the L-alanine containing construct, peptide **3**. In this case the peptide was insoluble beyond 100  $\mu\text{M}$ . At 100  $\mu\text{M}$ , the peptide sediments as a mixture of species of average MW 5999.33 ( $2.3 \times$  monomer). In striking contrast to the L-Ala substitution in peptide **3**, peptide **4**, with D-Ala at position 9, was highly soluble and sedimented as a stable trimeric species at 20, 200, and 1000  $\mu\text{M}$  (see Figure 3). In the screening process that led to the discovery of the **BBAT1** sequence,<sup>13</sup> the hinge residue was originally an L-cysteine residue capped with an *S*-methyl group. In the previous study, glycine was substituted for the L-Cys-SMe residue to improve the low solubility of the peptide. Glycine is a flexible amino acid that can attain backbone dihedral angles ( $\phi, \psi$ ) not accessible to substituted L-amino acids. Therefore, it was believed that the glycine hinge may have improved the solubility of the **BBAT1** peptide by allowing the  $\alpha$ - and  $\beta$ -domains to fold with the least amount of influence from the hinge residue. Thus, the AUC data for peptide **3** reconfirms that L-amino acid backbone dihedral angles may not be accommodated in the trimer fold and the data for peptide **4** suggest that the glycine loop in the folded trimer has dihedral angles that overlap with those favored in D-amino acids. Other D-amino acid hinge residues may also be able to stabilize the

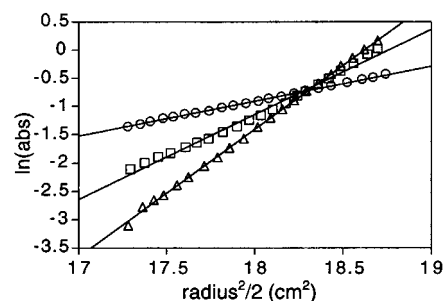


**Figure 4.** AUC data for peptide **7** (D-Asp) at 20  $\mu\text{M}$  (○), 100  $\mu\text{M}$  (□), and 500  $\mu\text{M}$  (Δ). The data are shown fit to a single ideal species model where  $\ln(\text{abs})$  vs  $r^2/2$  yields a straight line. Absorbance was monitored at 235 (20  $\mu\text{M}$ ), 246 (100  $\mu\text{M}$ ), and 290 nm (500  $\mu\text{M}$ ).

desired conformation. We explored this possibility by incorporating other D-residues with varying side chain functionality at this position in peptides **5–11**.

#### Effect of Hinge D-Amino Acid Side Chain: Neutral Polar.

Peptides **5** and **6** incorporate the neutral polar side D-amino acids asparagine and serine. Peptide **5** was insoluble above 100  $\mu\text{M}$ . At that concentration the peptide sediments as a mixture of primarily monomeric species with some oligomeric species. It appears that introduction of the asparagine side chain prevents the folding and stable oligomerization of the peptide that results in precipitation. Asparagine is known to occupy conformations not allowed in other nonglycyl residues. The favored dihedral angles for the residue may not overlap well with those required to allow stable trimer formation.<sup>24,25</sup> Peptide **6**, with D-Ser, was soluble at higher concentrations and sedimented as a trimeric species at both 100 and 500  $\mu\text{M}$ . However, the peptide only sedimented as a single ideal species at 500  $\mu\text{M}$ . This result suggests that the neutral polar serine side chain can be accommodated in the trimer fold but that the resulting structure is not as stable as the D-Ala or Gly hinge trimers in peptides **4** and **BBAT1**.

#### Effect of Hinge D-Amino Acid Side Chain: Polar Charged.

Peptides **7**, **8**, and **9** incorporated the polar charged amino acids D-aspartic acid, D-arginine, and D- $\alpha, \beta$ -diaminopropionic acid (D-Dap). While these amino acids introduce charge into the hinge, it is again interesting to note that these substitutions constitute fairly small changes to the chemical structures of peptides **4**, **5**, and **6**. Peptide **7**, with D-Asp, sediments as a single ideal trimeric species at 500  $\mu\text{M}$ . Interestingly, this peptide exists as a mixture of species at 100  $\mu\text{M}$  (average MW 5556.50,  $2.1 \times$  monomer) and is completely monomeric at 20  $\mu\text{M}$  (Figure 4). These results indicate that the placement of a negatively charged D-residue in the hinge can be tolerated but that its presence compromises the affinity for the peptide trimer, making it only stable at higher concentrations. It is possible that charge repulsion between aspartate carboxylates of the individual monomers or burial of the carboxylates in a hydrophobic environment weakens the association. The aspartic acid side chain may partially offset these destabilizing effects by providing some other stabilizing interaction such as N-terminal helix capping<sup>26</sup> or a hydrogen-bonded network between the carboxylates or with other groups in the peptide.

(24) Ravichandran, V.; Subramanian, E. *Int. J. Peptide Protein Res.* **1981**, *18*, 121–126.

(25) Srinivasan, N.; Anuradha, V. S.; Ramakrishnan, C.; Sowdhamini, R.; Balaram, P. *Int. J. Peptide Protein Res.* **1994**, *44*, 112–122.

(26) Aurora, R.; Rose, G. D. *Protein Sci.* **1998**, *7*, 21–38.

Peptides **8** and **9** contain positively charged D-amino acids. Unlike peptide **7**, neither of these peptides are able to associate to a stable trimeric species at 500  $\mu\text{M}$ . Peptide **8** (D-Dap) does exist as a single, monomeric species at 100  $\mu\text{M}$  and both peptides increase their average molecular weight with increasing concentration. Therefore, although the D-amino acid dihedral angles promote oligomerization, the positive charges are greatly destabilizing to the oligomeric state. This may occur as a result of charge repulsion between monomers, as a result of burial of the highly polar side chains in a hydrophobic environment, or as a result of the positive charges interfering with the negatively charged C-terminal helix capping sequence (Asp10-Glu11)<sup>16,26</sup> and opposing the natural helix dipole.<sup>27</sup>

#### Effect of Hinge D-Amino Acid Side Chain: Hydrophobic.

Peptides **10** and **11** incorporate hydrophobic groups of D-leucine and D-phenylalanine into the hinge. Given the destabilizing effects of the polar side chains, it was expected that these residues might permit trimer formation and perhaps result in a more stable structure. Interestingly, both peptides appear to sediment as tetrameric species. Peptide **10** (D-Leu) does not sediment as a single ideal species but rather exists as a mixture of species of average molecular weight greater than four times the monomer. Peptide **11** (D-Phe), however, does sediment as a single species and appears to be forming discrete tetramers at 20, 100, and 500  $\mu\text{M}$ . It may be possible that these bulky side chains expand the hydrophobic core of the structure sufficiently such that the most efficient packing of the hydrophobic groups is attained in the tetrameric state. Interestingly, the aliphatic leucine side chain fails to afford an oligomer with discrete association properties. A similar effect has been observed with helix bundle assemblies.<sup>28</sup>

**Structural Analysis by CD.** The results from analytical ultracentrifugation reveal that the hinge conformation, side chain polarity, and size are all important factors in controlling the extent of oligomerization of the **BBAT1** peptides. To evaluate the secondary structural content and stability of the **BBAT1** peptide oligomers, concentration and temperature-dependent CD spectroscopy was carried out. The CD spectrum of the parent peptide **BBAT1**, which contains the glycine hinge, is characteristic of a highly helical structure, and the concentration and temperature-dependent data indicated that the peptide had a high affinity for the trimeric state and that the oligomer was cooperatively folded.<sup>13,14</sup> While it is possible that the DapBz chromophore may be contributing to the observed CD signal, we are focusing on the relative effects of the sequence modifications on the trends observed in the concentration and temperature-dependent spectra. The AUC screen confirmed that peptides **4**, **6**, **7**, and **11** were able to form stable trimeric or tetrameric species. These peptides were therefore studied by concentration and temperature-dependent CD spectroscopy to probe the effect of the different hinge substitutions on the integrity of the quaternary structures.

Peptide **4** (D-Ala hinge) was a discrete trimer at all concentrations evaluated by AUC and was found to be most similar to **BBAT1** by AUC. If the glycine hinge of **BBAT1** allows the proper dihedral angles to be achieved in the folded trimer, then the D-Ala residue may actually enforce the proper geometry and

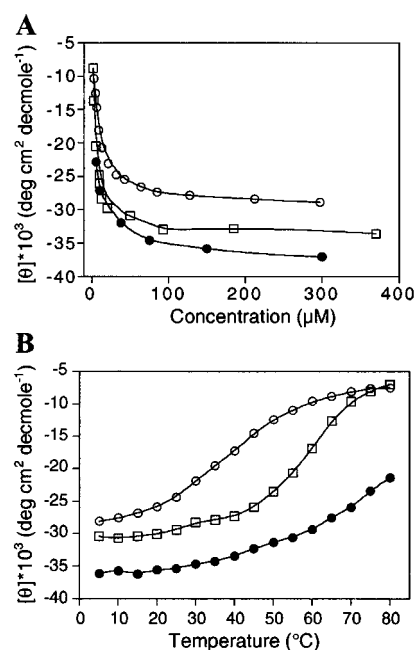


**Figure 5.** Concentration (A) and temperature (B) dependence of  $[\theta]_{222\text{nm}}$  for peptides **4** ( $\square$ ), **11** ( $\bullet$ ), and **BBAT1** ( $\circ$ ). Experiments performed in pH 7.0, 50 mM phosphate buffer. Temperature-dependent experiments were performed with 50  $\mu\text{M}$  peptide and concentration dependent experiments were performed at 5 °C. Lines are drawn for clarity.

stabilize the trimer structure. The concentration and temperature dependence of the CD spectra of peptide **4** at 222 nm are shown in Figure 5. The concentration-dependent data (Figure 5A) confirm that the helical structure of peptide **4** is enhanced relative to **BBAT1** and the temperature-dependent data (Figure 5B) reveal that the folded structure at 50  $\mu\text{M}$  is more stable to thermal denaturation and is perhaps more cooperatively folded than **BBAT1**. In fact, the midpoint of the melting transition appears to be more than 20 degrees higher in peptide **4** (64 °C) than in **BBAT1** (40 °C). It is important to note that at the highest temperatures and lowest concentrations, presumably where the peptides are monomeric, the residual CD signal for both peptides is almost identical.

The structure and stability of the other D-amino acid hinge peptides that form discrete oligomers was evaluated by a similar analysis. Of the polar amino acids incorporated into the trimer sequence, the D-Ser and D-Asp residues allowed stable trimer formation. Concentration-dependent CD analysis of peptides **6** (D-Ser) and **7** (D-Asp) show that the peptides have as high or a higher degree of secondary structure than **BBAT1** at concentrations where the peptides are trimeric (Figure 6). The transition to the more structured oligomeric form is, however, less sharp than in either the **BBAT1** or the D-Ala hinge peptide **4**. These results imply that although these D-amino acids are supporting a high degree of helical structure, the presence of the polar side chains weakens the association to the trimer form. This result is supported by the temperature-dependent CD spectra of peptides **6** and **7**. At 50  $\mu\text{M}$ , both peptides have melting transition midpoints well below that of peptide **4** (**6**, 35 °C; **7**, 34 °C; and **4**, 64 °C).

The peptides with hydrophobic D-amino acids (**10** and **11**) were found to form tetrameric oligomers by AUC. However, only peptide **11** formed stable, discrete oligomers. The CD analysis of peptide **11** is shown in Figure 5. The peptide exhibits

(27) Branden, C.; Tooze, J. *Introduction to Protein Structure*; Garland: New York, 1991.

(28) Betz, S. F.; DeGrado, W. F. *Biochemistry* **1996**, *35*, 6955–6962.

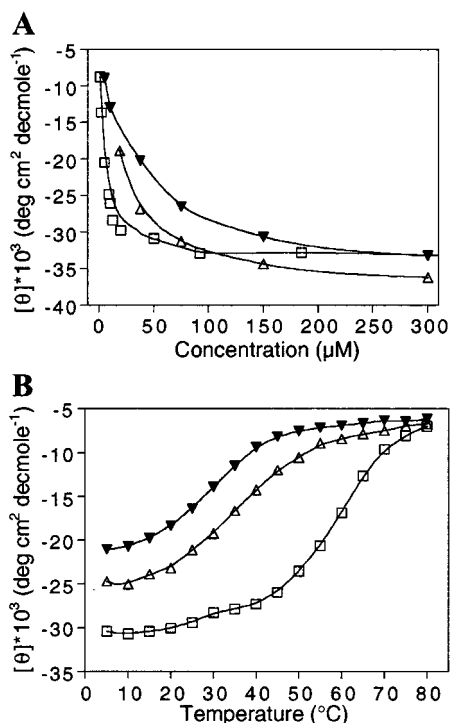


**Figure 6.** Concentration (A) and temperature (B) dependence of  $[\theta]_{222\text{nm}}$  for peptides **4** ( $\square$ ), **6** ( $\Delta$ ), and **7** ( $\blacktriangledown$ ). Experiments performed in pH 7.0, 50 mM phosphate buffer. Temperature-dependent experiments were performed with 50  $\mu\text{M}$  peptide and concentration dependent experiments were performed at 5  $^{\circ}\text{C}$ . Lines are drawn for clarity.

a higher degree of helicity than both **BBAT1** and peptide **4** (D-Ala) at all concentrations and was not completely denatured by 80  $^{\circ}\text{C}$ . Both of these findings suggest that peptide **11** forms a tetrameric structure that is stabilized relative to the original **BBAT1** trimer structure.

## Discussion

The oligomerization of the **BBAT1** peptide is a direct result of the truncation of the loop of **BBA5** from three amino acids to a hinge of one amino acid. Whereas the loop is a passive, connecting element that allows the  $\alpha$  and  $\beta$  elements of secondary structure to interact, the truncated hinge of the trimer appears not only to prevent the two elements of structure from interacting in a stable monomer structure, but also orients them in a fashion that allows for discrete intermolecular interactions. It is not surprising then, that this portion of the **BBAT1** sequence is highly sensitive to alteration. This study illustrates the sensitive nature of the hinge of the **BBAT1** peptide and describes some of the requirements for proper folding of the trimer structure. In addition, it was discovered that the hinge residue can be exploited to control the extent of oligomerization and the stability of association.

Peptides **2**, **3**, and **4** ( $\beta$ -, L- and D-alanine) differ very little from **BBAT1** and from each other in their chemical structures. However, only the conformational preferences of the D-alanine residue allow for stable trimer formation. In fact, it appears that the restriction of the dihedral angles of the hinge residue to those available to D-amino acids enhances the helicity of the peptide structure and the stability of the trimer. The side chain

of the D-amino acid placed at the loop can also restrict the accessible conformations available to the peptide such that the desired fold is not attained. For example, in peptide **5**, the D-Asn enforces a geometry that does not permit stable trimer formation and results in uncontrolled aggregation and precipitation. In the development of alternate oligomeric  $\beta\beta\alpha$  peptides, it may be possible to exploit other amino acids with distinct conformational preferences to select for or to preclude specific oligomeric states.

The chemical characteristics of the different side chain substitutions to the D-amino acid hinge also have a dramatic effect on the structure and oligomeric state of these  $\beta\beta\alpha$  peptides. The analysis of these substitutions also provides information regarding the chemical environment of the hinge in the folded trimer. The destabilizing effects of incorporating polar amino acids implies that the hinge residue is in contact with important hydrophobic groups. The positively charged side chains of peptides **8** and **9** may also be interfering with the helical structure of the monomer by opposing the helix dipole or interacting unfavorably with the acidic N-terminal helix capping sequence. It is also possible that, in the folded oligomer, the side chains are brought close in space and that the proximity of the charged groups is destabilizing to the quaternary structure. We are evaluating whether these polar interactions can be harnessed to stabilize dimeric or heterooligomeric structures.

The hydrophobic side chains of peptides **10** and **11** (D-Leu and D-Phe) result in the formation of tetrameric oligomers. While the D-Leu substitution appears to cause aggregation beyond a tetramer, the D-Phe loop of peptide **11** stabilizes a discrete structure. This tetrameric oligomer is stabilized relative to the trimer structures of peptides **4** and **BBAT1**. The shift to the tetramer may be a result of the larger bulk of the Leu and Phe side chains while the increased stability of the tetramer would be expected as a result of the larger volume of the buried hydrophobic groups.

These results illustrate the important roles that the hinge residue plays in the transformation of the monomeric BBA to the trimeric **BBAT1** and to higher order oligomers. These alternate oligomeric states are achieved through a combination of the conformational requirements of the hinge residue as well as the size and chemical nature of the side chain of the hinge residue. While the peptides analyzed in this study reveal that monomer, trimer, and tetramer are accessible, many alternate hinge amino acids could be combined with substitutions to other parts of the peptide sequence to create dimeric and higher order oligomers as well as novel heterooligomers. These structures would expand the collection of synthetic peptide scaffolds available for structural and functional studies and would provide insight into the forces which play key roles in protein–protein interactions.

**Acknowledgment.** We would like to thank Adam Mezo for helpful discussions. This research was supported by NSF grant CHE-9996335. The Multiuser Facility for the Study of Complex Macromolecular Systems (NSF-0070319) is also gratefully acknowledged.

JA016991D